The American Journal of Pathology, Vol. 173, No. 3, September 2008

DOI: 10.2353/ajpath.2008.080175

Molecular Pathogenesis of Genetic and Inherited Diseases

Amyloid Plaque and Neurofibrillary Tangle Pathology in a Regulatable Mouse Model of Alzheimer's Disease

Jennifer B. Paulson,* Martin Ramsden,* Colleen Forster,† Mathew A. Sherman,* Eileen McGowan,‡ and Karen H. Ashe*,§

From the Departments of Neurology and Laboratory Medicine and Pathology,† University of Minnesota, Medical School, Minneapolis, Minnesota; the Geriatric Research Education and Clinical Center,§ Veterans Administration Medical Center, Minneapolis, Minnesota; and the Department of Neuroscience,‡ Mayo Clinic Jacksonville, Jacksonville, Florida*

Transgenic mouse models that independently express mutations in amyloid precursor protein (APP) and tau have proven useful for the study of the neurological consequences of amyloid-β (Aβ) plaque and neurofibrillary tangle pathologies. Studies using these mice have yielded essential discoveries with regard to specific aspects of neuronal dysfunction and degeneration that characterize the brain during Alzheimer's disease (AD) and other age-dependent tauopathies. Most recent transgenic studies have focused on the creation of regulatable models that allow the temporal control of transgene expression. To study a more complete model of AD pathology, we designed a new regulatable transgenic mouse that harbors both APP and tau transgenes. Here, we present a novel transgenic mouse model, rTg3696AB, which expresses human APP_{NLI} and tau_{P301L} driven by the CaMKII promoter system. Subsequent generation of Aβ and 4R0N tau in the brain resulted in the development of three neuropathological features of AD: Aβ plaques, neurofibrillary tangles, and neurodegeneration. Importantly, transgene expression in these mice is regulatable, permitting temporal control of gene expression and the investigation of transgene suppression. *(Am J Pathol 2008, 173:762–772; DOI: 10.2353/ajpath.2008.080175)*

The diagnosis of Alzheimer's disease (AD) is confirmed after postmortem examination and is dependent on the identification of senile plaques and neurofibrillary tangles (NFTs). In addition to neuronal loss, these extracellular deposits of β-amyloid (Aβ) peptide and intraneuronal accumulations of hyperphosphorylated tau represent the histological hallmarks of this devastating neurological disorder.[1] For almost a century, AD researchers believed that accumulation of insoluble Aβ and tau species represented a purely detrimental event in the brain. However, recent studies have questioned this assumption and confirmed that the true pathological relevance of these neuronal lesions is still not completely understood.

Experiments using transgenic mice have been particularly valuable for independently studying the progression of plaque and NFT pathologies. Studies using mice that express amyloid precursor protein (APP) have provided significant insights regarding the contribution of Aβ plaques to brain dysfunction. In APP transgenic mice, plaques are associated with dendritic spine loss, neuritic dystrophy, neuronal death, and abnormal axonal morphology,[2–8] which lead to a subsequent disruption of synaptic integration.[9] Although it is believed that Aβ plaques play a fundamental role in the pathology of AD, their precise contribution to neurodegeneration is unclear. Interpreting the significance of amyloid plaques has been complicated by advances in the study of Aβ, their primary component. It is now known that Aβ exists in many distinctly different forms. These include monomers of Aβ, low- and high-molecular weight soluble Aβ oligomers, Aβ-derived diffusible ligands, amyloid pores, protofibrils, and fibrils.[10–17] In turn, these specific Aβ species have been shown to exert a myriad of neurotoxic and dysfunctional effects *in vitro* and *in vivo*.[17,18] Moreover, recent work suggests the cumulative impact of Aβ species on the brain is governed by an equilibrium be-

Supported by the National Institutes of Health (grant AG26252 to K.H.A.), the National Institute on Aging (grant AG020216 to E.M.), the John Douglas French Alzheimer's Foundation (to M.R.), and by gifts from E.W. and A.M. Tulloch and B. Grossman (to K.H.A.).

J.B.P. and M.R. contributed equally to this study.

Accepted for publication June 11, 2008.

Address reprint requests to Dr. Karen H. Ashe, Department of Neurology, University of Minnesota Medical School, 420 Delaware St. SE, MMC 295, Minneapolis, MN 55127. E-mail: hsiao005@umn.edu.

tween soluble and fibrillar Aβ, and the subsequent deposition of Aβ as senile plaques.[19]

Equally, transgenic models expressing mutated forms of human tau have furthered our understanding of NFT formation and associated pathologies.[20–25] Previously, we created rTg4510 (tau_{P301L}), a regulatable model of human tauopathy that is characterized by the age-dependent development of memory impairment, NFTs, and neuronal loss.[26] Recent studies in these mice showed that NFT pathology continued after substantial transgene suppression.[27] Moreover, NFT pathology progressed concurrently with a significant improvement in retention of spatial reference memory. These surprising data suggested that NFTs were not primarily responsible for cognitive impairment in rTg4510 and may in fact represent an attempted neuroprotective sequestration of tau. The specific form of tau responsible for inducing dysfunction that precedes NFT pathology remains to be determined.

Most recent transgenic studies have focused on the creation of regulatable models that allow the temporal control of transgene expression.[28] Here, we present a novel transgenic mouse model, rTg3696AB, which express human APP_{NLI} and tau_{P301L} driven by the CaMKII promoter system. These mice are characterized by deposition of amyloid plaque and tau NFT pathologies that are accompanied by tissue atrophy and neuronal loss. In addition, rTg3696AB were created as regulatable transgenic mice to incorporate temporal control of transgene expression and allow investigation of the effect of transgene suppression.

Materials and Methods

Generation of Mice

Briefly, our methods for generating rTg3696AB mice used a system of responder and activator transgenes (r stands for regulatable, and indicates the presence of responder and activator transgenes; absence of r signifies responder-only lines). Mice expressing the activator transgene were derived from a generous gift of Dr. Eric Kandel at Columbia University, New York, NY[28] and successively backcrossed at least five times onto a 129S6 background strain. Responder mice were maintained in the FVB/N strain. Mice expressing the Tg3696A and Tg3696B transgenes were identified by Southern blot of DNA restricted with *Eco*RI and probed with the ~1.3-kb *Xba*I-*Eco*RI fragment of the MoPrp.XhoI minigene vector. Animals were identified as being from the Tg3696A line if they contained two bands at 3.7 kb and 2.9 kb and from the Tg3696B line if they contained a band at 4.5 kb. Tg3696A and Tg3696B lines were mated together to create Tg3696AB responders, containing both RFLP patterns. Tg3696AB responders were identified by Southern blot and were obtained in a Mendelian ratio of 1 in 4. The Tg3696AB responders were subsequently mated to the activator TgCK-tTA line and pups positive for all three transgenes were screened by polymerase chain reaction using the primer pairs 5′-GATTAACAGCGCATTAGAGCTG-3′ and 5′-GCATATGATCAATTCAAGGCCGATAAG-3′ for the activator transgene, 5′-TGAACCAGGATGGCTGAGCC-3′ and 5′-TTGTCATCGCTTCCAGTCCCCG-3′ for the tau transgene, and 5′-AAGCGGCCAAAGCCTGGAGGGTGGAACA-3′ and 5′-GTTGAGCCTGTTGATGCCCG-3′ for the APP transgene. Pups positive for all three transgenes were screened by Southern blot by the method described above to identify the mice that contained both A and B alleles.

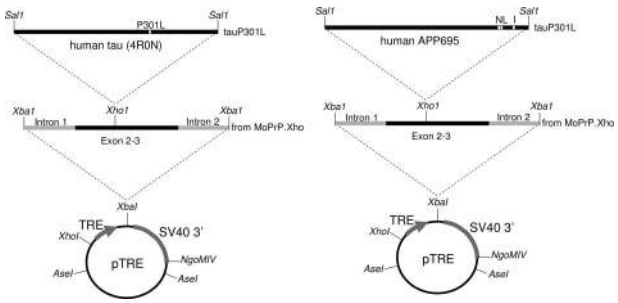

Figure 1. The tau_{P301L} and APP_{NLI} responder transgene constructs.

The APP and tau transgenes are diagrammed in Figure 1. The tau transgene was previously described.[27] To generate the APP transgene, a $Val_{717} \rightarrow Ile_{717}$ mutation (*London*) was introduced using standard site-directed mutagenesis techniques into a previously created APP cDNA encoding 695 amino acids with mutations at $Lys_{670} \rightarrow Asn_{670}$, $Met_{671} \rightarrow Leu_{671}$ (*Swedish mutation*) (numbering is based on a 770-codon open reading frame). The resultant APP_{NLI} transgene driven by TRE was placed in the context of the mouse prion protein gene (*prnp*) transcribed but untranslated sequences, which were derived from the MoPrP.Xho expression vector, a generous gift of Dr. D. Borchelt, (Dept. Neuroscience, University of Florida, FL).[29] First, the *Sal*I fragment of a previously created APP_{NL} transgene (starting 10 bases upstream of the start methionine and extending four bases downstream of the stop codon),[30] was inserted into Bluescript (Stratagene, Inc., La Jolla, CA) to introduce the *London* mutation. Next, the *Sal*I fragment of the resultant APP_{NLI} construct was inserted into the unique *Xho*I site of MoPrP.Xho to generate *prnp*.APP_{NLI}. Third, the *Xba*I fragment of *prnp.*APP_{NLI}, including partial sequences of *prnp* introns 1 and 2, along with exons 2 to 3, and the APP_{NLI} open reading frame, was cloned into the unique *Xba*I site in the inducible expression vector pTRE (Clontech, Inc., Palo Alto, CA), resulting in the plasmid, pTRE.prnp.APP_{NLI}. The resultant DNA was digested with *Xho*I and *Ngo*M IV enzymes, fractionated, and purified by electroelution followed by organic extraction. Purified fragments containing modified APP and tau transgenes were co-introduced by microinjection into the pronuclei of donor FVB/N embryos, by standard techniques. All experiments described in this report were conducted in full accordance with the Association for Assessment and Accreditation of Laboratory Animal Care and the Institutional Animal Care and Use Committee guidelines, with every effort made to minimize the number of animals used. Multiple mice were generated during characterization of this new line. All figures describe specific observations for $n = 3$ mice per group, per age.

In Situ *Hybridization*

Sagittal cryostat sections (15 μm) were fixed in 4% paraformaldehyde, dehydrated, and hybridized with a human tau-specific oligomer (5′-CTTTCAGGCCAGCGTCCGTGTCACCCTCTTGGTC-3′) or human APP-specific oligomer (5′-TTGATGATGAACTTCATATCCTGAGTCATGTCGGAATTC TRANSGENIC ATC-3′) 3′-end labeled with α^{35}S dATP. Sections were hybridized at 37°C overnight in buffer containing 4× standard saline citrate, 1× Denhardt's solution, 50% v/v deionized formamide, 10% w/v dextran sulfate, 200 mg/μl herring sperm DNA, and 0.03% β-mercaptoethanol. Control sections were hybridized in the presence of a 50- to 100-fold molar excess of unlabeled oligonucleotide. After hybridization, the sections were stringently washed three times with 1× standard saline citrate at 50°C, dehydrated, and exposed to Kodak Biomax film (Eastman-Kodak, Rochester, NY) for 1 to 4 days. Slides were developed using Kodak D-19 and fixed using Ilford Hypam Calumet Photographic (Bensenville, IL) fixative, and counterstained with Toluidine blue.

Biochemistry

Mouse brain tissue for biochemical studies was rapidly dissected then quickly frozen in isopentane for storage at −80°C. To generate forebrain lysates, olfactory bulbs, corticolimbic and subcortical brain stem structures, and cerebellum were all removed. Frozen hemi-forebrains were subjected to an extraction protocol, as described previously.[17] All extraction solutions were used at 4°C and contained protease inhibitor cocktail, phenylmethanesulfonyl fluoride, phenenthroline monohydrate, and phosphatase inhibitor cocktails I and II (all from Sigma, St. Louis, MO), at a final dilution of 1:100. To estimate total levels of transgenic tau protein corrected (Bradford assay) brain extracts were diluted in reducing sample buffer, electrophoresed on 10% Tris-HCl gels (Bio-Rad, Hercules, CA), then transferred onto 0.45-μm polyvinylidene difluoride membranes (Millipore, Bedford, MA). To estimate transgenic APP, samples were electrophoresed on 10 to 20% Tris-Tricine gels, then transferred onto 0.2-μm nitrocellulose membranes (Bio-Rad). Briefly, blots were processed with primary antibodies 6E10 (1:2000, recognizes human APP; Signet Laboratories, Dedham, MA) and Tau-5 (1:5000, recognizes mouse and human tau; Biosource, Camarillo, CA), α-tubulin (Sigma), and visualized using enhanced chemiluminescence reagents (Pierce, Rockford, IL) followed by exposure onto hyperfilm (Kodak).

Immunohistochemistry (IHC)

Hemi-brains were immersion-fixed in 10% formalin for 24 to 48 hours and embedded in paraffin. Serial sections were cut at 5 μm using a microtome, mounted onto CapGap slides Fisher Scientific (Pittsburgh, PA), and rehydrated according to standard protocols. Mounted slides were pretreated with a 6.0 pH citrate buffer in a Black & Decker (Owings Mills, MD) steamer for 30 minutes with a 20-minute cool down. Standard 2-day immunostaining procedures using peroxidase-labeled streptavidin and diaminobenzidine chromagen on an automated TechMate Dako (Glostrup, Denmark) 500 capillary gap immunostainer were used. Hematoxylin counterstaining was used to provide cytological detail. Hematoxylin and modified Bielschowsky silver staining were performed using standard histological techniques. All primary antibody concentrations were titered to provide optimal staining. Antibodies used were MC-1 (amino acids 7 to 9 and amino acids 326 to 300, 1:1000; Dr. P. Davies), CP-13 (pSer^{202}, 1:2000; Dr. P. Davies, Albert Einstein College of Medicine, NY), AT-8 (pSer^{202} /pThr^{205}, 1:4000; Innogenetics, Alpharetta, GA), PG-5 (pSer^{409}, 1:200; Dr. P. Davies), 6E10 (Aβ amino acids 3 to 8, 1:5000; Signet), 4G8 (Aβ amino acids 18 to 22, 1:3000; Signet), A$\beta_{x\text{-}40}$ (1:500; Calbiochem. La Jolla, CA), A$\beta_{x\text{-}42}$ (1:50; Calbiochem), 22C11 (APP amino acids 66 to 81, 1:800; Boehringer Mannheim. Indianapolis, IN), NeuN (1:4000, Chemicon), GFAP (1:20,000; DAKO, Carpinteria, CA). No positive labeling was observed for pathological tau epitopes in nontransgenic mice.

Results

Generation of a Regulatable Transgenic Model Expressing APP$_{NLI}$ and Tau$_{P301L}$

To provide a disease model characterized by Aβ plaque and NFT pathology we created a novel transgenic mouse expressing human APP and tau. To facilitate Aβ42 production, we expressed APP harboring the *Swedish* mutations (K670N and M671L) at the β-secretase site and the *London* mutation (V717I) at the γ-secretase site (APP$_{NLI}$).[31,32] To achieve concurrent NFT pathology, we also expressed human 4R0N tau containing a mutation in tau that has been linked to hereditary tauopathies (P301L; Hutton et al,[38] 1998). To obtain levels of Aβ and tau expression required to achieve plaque and NFT development within the first year of life, two independent lines of mice, rTg3696A and rTg3693B, harboring co-integrated APP and tau transgene arrays at different insertion sites, were identified by Southern blot (Figure 2A) and mated together to create rTg3696AB mice.

To enable the ultimate goal of studying the dependence of pathology on continued transgene expression, we engineered a regulatable transgenic model. This approach utilizes a system of responder and activator transgenes. Responder mice harboring TRE-APP$_{NLI}$ and TRE-tau$_{P301L}$ transgenes are bred with activator mice, which express the tet-off tTA open reading frame placed downstream of CaMKII promoter elements.[33] This system has been shown to result in expression from the TRE that is restricted to forebrain structures and is predominantly restricted to neuronal cell types.[26,28] Mice harboring responder or activator transgenes were bred to generate trigenic progeny containing all three transgenes (rTg3696AB, where r stands for regulatable) (Figure 2B). Consistent with this, transgenic mRNA expression in bigenic mice was primarily restricted to neuronal cells in the forebrain (Figure 2C). The highest

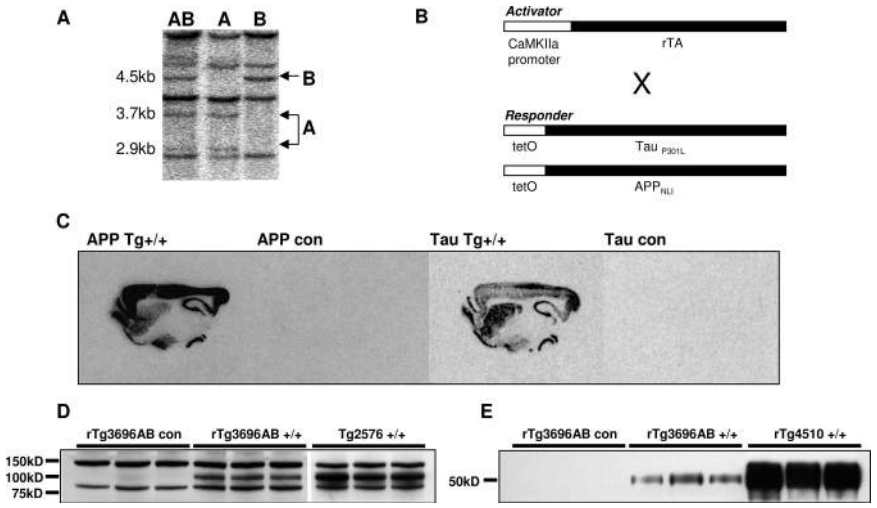

Figure 2. Generation of the regulatable transgenic mouse model rTg3696AB. **A:** Mice expressing both Tg3696A and Tg3696B were identified by Southern blot. **B:** Activator mice expressing the forebrain-specific neuronal CAMKII promoter were crossed with responder mice expressing both APP_{NLI} and Tau_{P301L} transgenes. **C:** Specific transgene expression in the forebrain was confirmed by *in situ* hybridization in rTg3696AB mice. **D** and **E:** Western blots confirmed transgenic protein expression in the forebrain of 11-month rTg3696AB mice. APP_{NLI} was detected using 6E10 and tau was detected after incubation with Tau-5 primary antibody. APP and tau transgene expression is compared to Tg2576 (APP) and Tg4510 (Tau) as positive controls, respectively.

expression was observed in the hippocampus and cortex. Transgenic mRNA was detectable throughout all fields of the hippocampal formation and in all layers of the cortex, except for lamina I, in which there are no cell bodies. To confirm transgenic protein expression, forebrains were subjected to an established extraction procedure and protein levels examined by Western blot.[17] We detected high levels (~3 units, 1 unit being equivalent to endogenous protein) of human full length APP in rTg3696AB brain that were estimated at approximately half the level found in Tg2576 mice (Figure 2D). In parallel, immunoblots revealed strong expression of tau_{P301L} (~3 units), which was measured as ~25% of that expressed in rTg4510 (Figure 2E).

Development of Amyloid Plaque Pathology

At 4 months of age a cohort of rTg3696AB were euthanized, brain tissue fixed, and subjected to IHC analyses. To examine APP expression, tissue was processed with 4G8, an antibody that recognizes amino acids 18 to 22 of the Aβ sequence. Brown diaminobenzidine reaction end product indicated strong expression throughout disease-relevant structures of the forebrain such as hippocampus and frontal cortex (Figure 3, A–C). Transgenic APP expression was especially strong in the hippocampus with dense somatic neuronal labeling of APP observed in CA1. Although 4G8 recognizes both endogenous mouse and transgenic human APP species, at the concentration used only weak staining was observed in simultaneously processed age-matched transgenic control tissue (Figure 3, D–F). To ensure that this positive labeling represented transgenic APP species, and not an intracellular accumulation of Aβ, we processed tissue with antibody 22C11 that recognizes APP amino acids 66 to 81. Consistent with the 4G8 results, prominent somatic labeling was observed in the rTg3696AB mice, indicating the expression of transgenic human APP (Figure 3, G–J).

We first detected Aβ plaque structures at 4 months of age that were restricted to the frontal cortex (Figure 3, K–P). As previously reported in Tg2576 and other APP transgenic lines, the first visible plaques were cored fibrillar deposits.[19,34–36] To confirm the content of the 4G8-positive plaques was dominantly Aβ, we conducted parallel experiments using $A\beta_{x\text{-}40}$- and $A\beta_{x\text{-}42}$-specific antibodies (Figure 3, L and M). Although these antibodies readily detected Aβ deposited as extracellular plaques, processing with $A\beta_{x\text{-}40}$ and $A\beta_{x\text{-}42}$ did not support the accumulation of intracellular Aβ in this model. As a further positive control, postmortem AD tissue supported the use of 4G8 to detect Aβ plaques (Figure 3N). In addition, an aged Tg2576 mouse with substantial amyloid load was processed in parallel to confirm the specificity of $A\beta_{x\text{-}40}$ and $A\beta_{x\text{-}42}$ antibodies (Figure 3, O and P).

Development of NFT Pathology

Early tau pathology was examined in 4-month rTg3696Aβ mice using a panel of antibodies directed at biochemical changes in tau that are associated with AD. Consistent with previous reports in AD and transgenic tau models,[23,26] the earliest positive labeling was observed with CP-13 and MC-1 that detect phosphorylation- and conformation-dependent epitopes, respectively (Figure 4). For CP-13, strong signal was observed throughout the hippocampus and cortex, with the most prominent labeling detected in the cell bodies and dendrites of CA1 hippocampal neurons (Figure 4). Processing with MC-1 revealed a population of positively labeled neurons in the CA1 but no somatic neuronal staining in the cortex (Figure 4). In addition, we used antibodies designed to test the presence of pretangles (accumulations of nonargyrophilic hyperphosphorylated tau in the neuronal cell body) in human tauopathies. At 4 months of age very few neurons were positively labeled with AT-8 or PG-5, indicating the early stage of tau pathology at this age (Figure 4). In parallel to Aβ studies, human tissue from a FTDP-17 subject with the tau_{P301L} mutation was included as a positive control (data not shown).[26]

Age-Dependent Progression of Amyloid Burden

Plaque pathology was examined in older animals. At 11 months of age IHC studies revealed prominent Aβ plaque

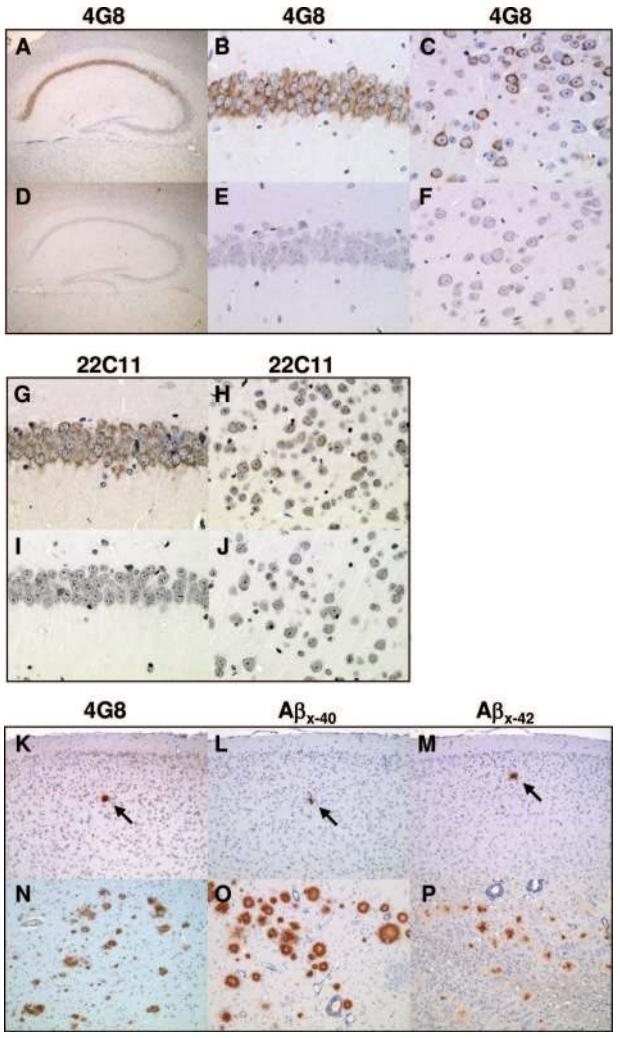

Figure 3. APP expression and Aβ plaque development in rTg3696AB mice. **A–C:** IHC studies with 4G8 confirm strong APP expression in the forebrain hippocampus of 4-month rTg3696AB$^{+/+}$ mice (**A**, hippocampus; **B**, CA1; **C**, frontal cortex) compared to age-matched nontransgenic littermates (**D–F**). Positive somatic labeling was shown to represent transgenic APP using antibody 22C11 (**G** and **I**, CA1; **H** and **J**, frontal cortex). Aβ plaques (**arrow**) were first observed in the frontal cortex at 4 months of age, as detected by 4G8 (**K**), $A\beta_{x\text{-}40}$ (**L**), and $A\beta_{x\text{-}42}$ (**M**). Human cortical tissue from an AD patient was processed in parallel as a positive control for detection of Aβ plaques using 4G8 (**N**). Serial sections of 24-month Tg2576 brain were used as positive controls for antibodies $A\beta_{x\text{-}40}$ (**O**) and $A\beta_{x\text{-}42}$ (**P**). Original magnifications: ×5 (**A**, **D**); ×10 (**K–P**); ×40 (**B**, **C**, **E–J**).

pathology in the brains of rTg3696AB mice (Figure 5). Substantial plaque deposition was observed in brain regions where expression of the CaMKII-driven transgene is highest, such as hippocampus and cortex. In the hippocampus, plaque deposition was most commonly observed in close proximity to the CA1 (Figure 5A). We also detected substantial numbers of Aβ plaques throughout the cortex (Figure 5B). Consistent with the use of the forebrain-specific promoter, no plaque deposits were detected in the cerebellum or brainstem at any age.

To investigate the rate of plaque deposition after substantial amyloid burden, pathology was measured at 13 months. Interestingly, IHC images showed a considerable increase in plaque pathology during this 2-month period (Figure 5). This observation was supported after IHC studies with both $A\beta_{1\text{-}40}$- and $A\beta_{1\text{-}42}$-specific antibodies (Figure 5). The increase in total amyloid load appeared to be dependent on an increase in both the number of plaques and the size of plaques detected. To further support these IHC observations, plaque deposition was further studied using Bielschowsky histology to detect insoluble β-sheet amyloid deposits (see below).

Age-Dependent Progression of Tau Pathology

To investigate the progression of tau pathology we examined the expression of pretangle-associated epitopes at 11 months. At this age we identified high numbers of neurons that were positively labeled for pathological biochemical changes in tau (Figure 6). As described previously,[23,26] we observed an age-dependent shift in CP-13 labeling from the neurites to the soma and increased somatic MC-1 labeling (data not shown). Moreover, at 11 months many hippocampal and cortical neurons were detected with pretangle antibodies AT-8 and PG-5 (Figure 6). In the hippocampus, pretangles were most commonly observed in the CA1 subdivision. To determine whether the observed accumulations of intracellular tau represented mature NFTs, we processed tissue sections histologically. The development of mature argyrophilic NFTs was confirmed at 11 months after traditional histological processing with Bielschowsky silver stain (Figure 7).

In parallel to measurements of amyloid burden we euthanized rTg3696AB mice at 13 months of age to estimate the progression of tau pathology at this age. Processing tissue with pretangle antibodies revealed a substantial increase in AT-8 and PG-5 deposits at 13 months of age. Because the majority of CA1 neurons stained positive for AT-8/PG-5 at 11 months the most prominent further increase in 13 months mice was observed in the CA3 subdivision (Figure 6A). The increase in pretangle epitope expression was more striking in the frontal cortex where staining was significantly increased in 13-month versus 11-month mice (Figure 6B). To extend the analysis of tau pathology, we examined the formation of mature NFTs by using a concurrent histological approach. The progression of NFT pathology detected with Bielschowsky was extremely consistent with pretangle data suggesting a substantial increase in NFT numbers between the ages of 11 and 13 months (Figure 7).

Age-Dependent Neurodegeneration

To study the neurodegenerative consequences of plaque and NFT pathology we processed tissue sections histologically. There was no obvious hippocampal cell loss in 11-month rTg3696AB mice versus age-matched nontransgenic controls. However, at 13 months there was a striking degree of neuronal loss (Figure 8). Representative images of hematoxylin and eosin stained tissue show age-dependent tissue atrophy and neuronal loss in both the hippocampus and cortex. The most severely affected hippocampal subdivisions were CA1 and the molecular layer of the dentate gyrus. At 13 months, low magnification images show tissue atrophy after substantial neuro-

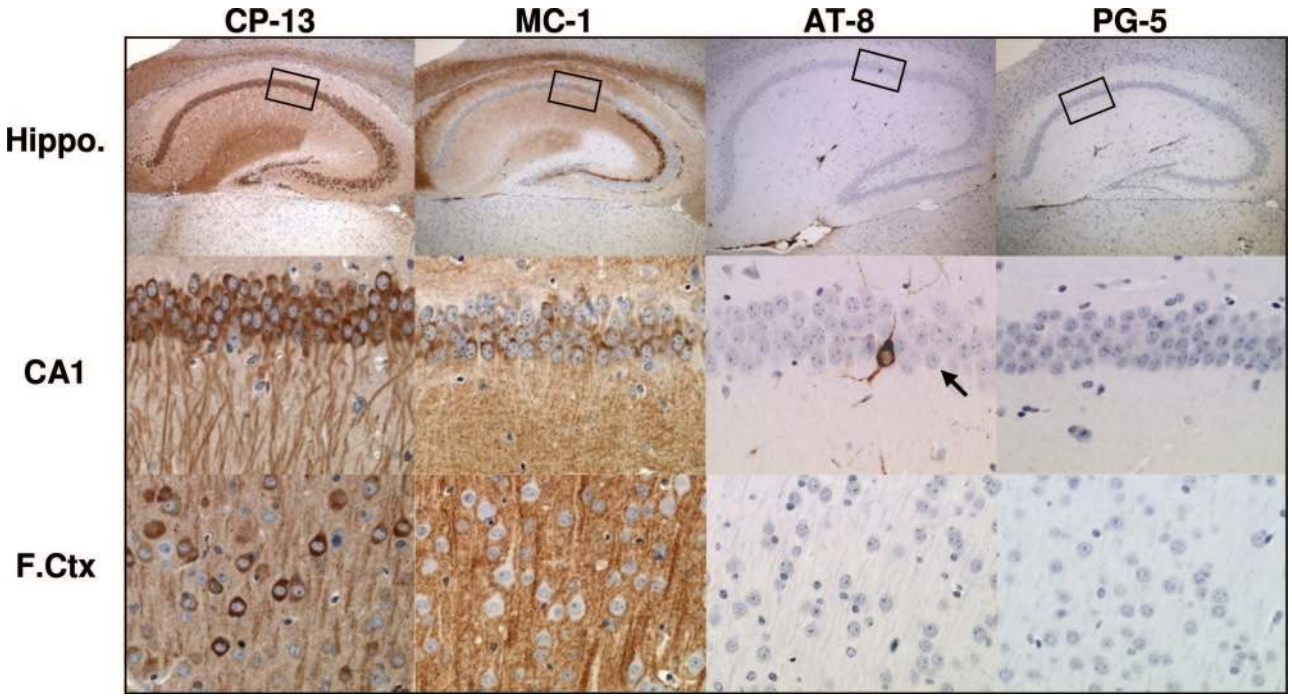

Figure 4. Accumulation of pathological tau species in rTg3696AB brain. At 4 months of age, IHC studies revealed abnormal tau conformation and phosphorylation in rTg3696AB hippocampus and frontal cortex. Enlarged images of hippocampal subdivision CA1 are shown in **middle** panel. At this age, neurons were positively labeled using antibodies directed at pathological epitopes dependent on changes in conformation (MC-1, amino acids 7 to 9 and amino acids 326 to 300) and phosphorylation (CP-13, $pSer^{202}$; AT-8, $pSer^{202}/pThr^{205}$; PG-5, $pSer^{409}$). Boxes indicate area shown at higher magnification. Rare AT-8-positive CA1 neuron indicated by **arrow**. Original magnifications: ×5 (**top**); ×40 (**middle**, **bottom**).

nal loss in the cortex. High magnification images of hematoxylin stained tissue indicated localized neuronal loss in the cortex after plaque deposition (Figure 8B). To supplement histological examination, tissue was incubated with antibodies NeuN and GFAP, to independently label neurons and glia, respectively. Consistent with our previous observations, substantial neuronal loss was observed between 11 and 13 months of age in the cortex and hippocampus, after labeling with neuron-specific antibody NeuN (Figure 9). These neurodegenerative changes were associated with a parallel increase in the number of reactive astrocytes detected with GFAP (Figure 9).

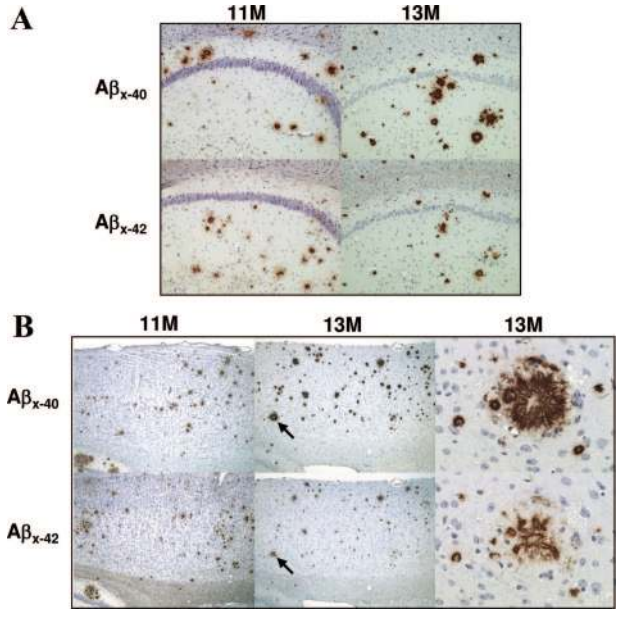

Figure 5. Age-dependent progression of plaque pathology. IHC images indicate substantial accumulation of Aβ plaque pathology in rTg3696AB mice between 11 and 13 months of age. Representative photomicrographs depict hippocampal (**A**) and cortical (**B**) pathology detected with $A\beta_{x-40}$ and $A\beta_{x-42}$. **Arrows** indicate specific plaques shown at high magnification. Original magnifications: ×10 (**A**); ×5 (**B**, low-power cortical images); ×40 (**B**, high-power plaque images).

Discussion

We have previously created mice that independently express human APP_{SWE} ($Tg2576^{30}$) and tau_{P301L} ($rTg4510^{26}$). These models have proven useful for studying specific aspects of neuronal dysfunctional and degeneration.[17,27] However, to study a more complete model of AD pathology we designed a new transgenic mouse harboring both APP and tau transgenes. Here, we present a novel transgenic mouse model, rTg3696AB, which expresses both human APP_{NLI} and tau_{P301L}. Subsequent generation of Aβ and 4R0N tau in the brain resulted in the development of three neuropathological features of AD: Aβ plaques, NFTs, and neurodegeneration. Importantly, transgene expression in these mice is regulatable permitting temporal control of expression.

To enhance $A\beta_{42}$ production, we expressed human APP harboring three mutations associated with early development of AD. To ensure transgenic APP was specifically expressed in the forebrain (and not also in the brainstem or peripheral organs,[35]) expression was driven by the CaMKII promoter system.[28] In addition to the

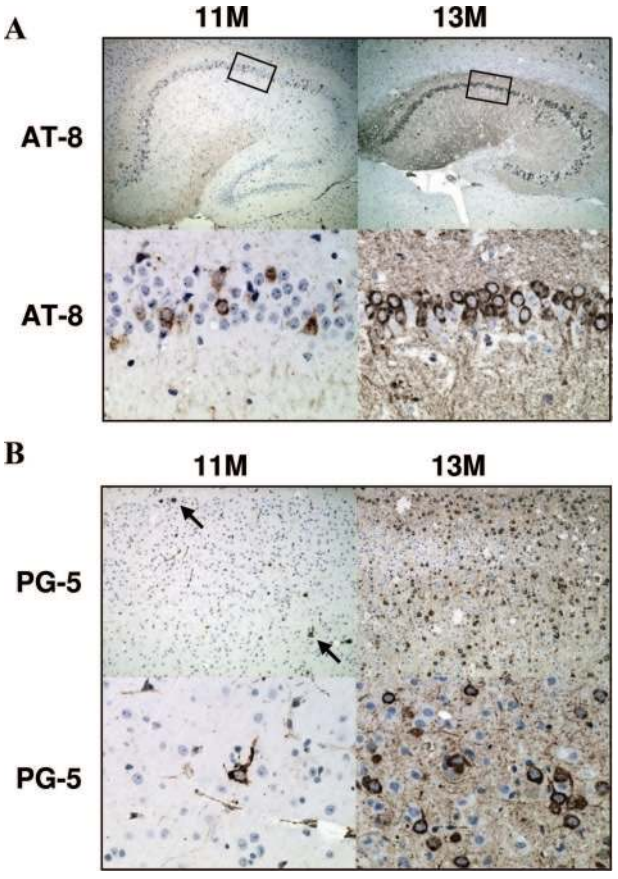

Figure 6. Age-dependent progression of tau pathology. Aberrant biochemical changes in tau were detected by IHC. Increased numbers of hippocampal and cortical neurons were positively labeled with antibodies that recognize pathological tau epitopes in 13-month versus 11-month mice. Representative images depict positive labeling with pretangle antibodies AT-8 (**A**) and PG-5 (**B**) in hippocampus and frontal cortex. Boxes indicate area shown at higher magnification. Original magnifications: ×5 (**A**, **top**); ×10 (**B**, top); ×40 (**A**, **B**, **bottom**). Arrows indicate PG-5 positive cortical neurons in 11-month old mice.

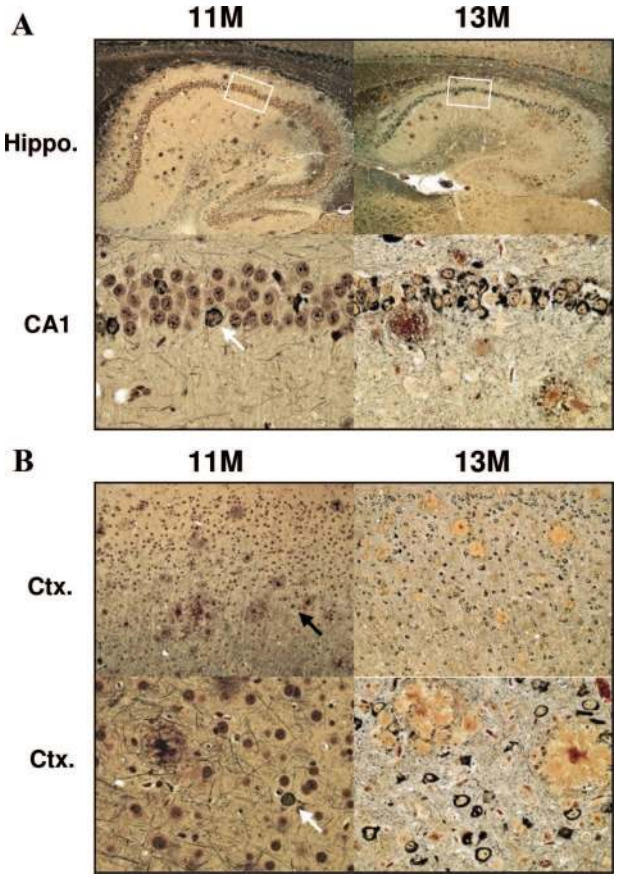

Figure 7. Progression of mature plaque and NFT pathology. Tissue was impregnated with Bielschowsky silver stain to visualize mature plaque and tangle pathology. **A:** Representative images are shown for hippocampus, including higher magnification of CA1 (**bottom**). **B:** NFT pathology was also evident in frontal cortex. NFT pathology can most clearly be observed in high-power images (**bottom**). Rare Bielschowsky-positive NFTs in 11-month brain highlighted with **arrow**. Boxes indicate area shown at higher magnification. Original magnifications: ×5 (**A**, **top**); ×10 (**B**, **top**); ×40 (**A**, **B**, **bottom**).

Swedish mutations (K670N and M671L) at the β-secretase site that characterize the Tg2576 model, rTg3696AB mice also harbor the *London* mutation (V717I) at the γ-secretase site. However, expression levels of transgenic APP in rTg3696AB brain were estimated at ~50% of those in Tg2576 mice. This lowered transgene expression served to highlight the power of incorporating the *London* mutation, and may also reflect an effect of mutant tau, consistent with a previous report that tau accelerated APP-related pathology.[37] Despite lower levels of human APP, plaque deposition was enhanced in rTg3696AB versus Tg2576 brain. In Tg2576, previous studies observed the first formation of Aβ plaques between 7 and 10 months of age.[35] After IHC processing, cored fibrillar deposits could be detected in rTg3696AB mice aged 4 months. Given the equal levels of transgenic APP in the cortex and hippocampus it is not clear why cortical plaque deposition precedes that in the hippocampus. By 11 months of age, substantial plaque deposition was observed in both the hippocampus and throughout the cortex. Consistent with previous reports, the rate of plaque deposition appeared to increase after initial accumulation as both the size and number of Aβ deposits were substantially augmented between 11 and 13 months of age.[35]

In rTg3696AB we expressed the same form of mutant tau that induced age-dependent NFT pathology in rTg4510. Both models express the P301L mutation in 4R0N human tau that has been linked to the development of hereditary tauopathy.[38] Similar to comparisons in APP, levels of transgenic human tau were substantially lower in rTg3696AB versus rTg4510 mice. Expression of P301L tau was estimated at ~25% of that previously described in rTg4510,[27] representing ~3 units of human tau to 1 unit of endogenous mouse tau. Perhaps not surprisingly, the age-dependent progression of tau pathology was attenuated in rTg3696AB versus rTg4510 mice. However, it is noteworthy that any tangle pathology developed at all, as mice expressing ~7 units of tau, driven by the same promoter, developed NFTs only at 20 months.[27] The acceleration of tangle pathology in rTg3696AB is likely enhanced by Aβ, supporting previous reports.[21,39] Consistent with the progression of disease in human brain, the earliest pathological epitopes of tau observed in rTg3696AB brain were dependent on changes in phos-

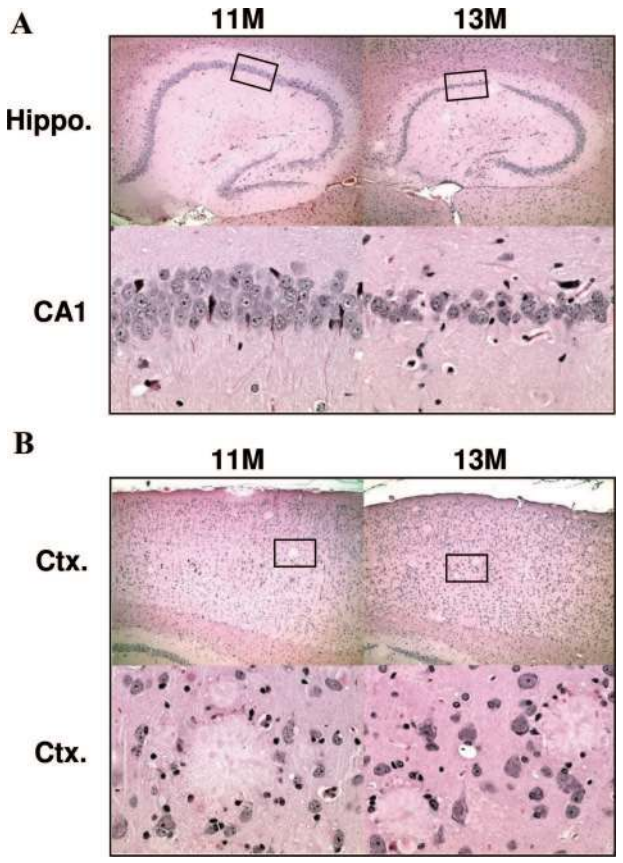

Figure 8. Tissue atrophy in aged rTg3696AB mice. Histological images indicate substantial loss of neurons in rTg3696AB mice between 11 and 13 months. Representative photomicrographs depict hippocampus (**top**) and cortex (**bottom**) after processing with H&E. Boxes indicate area shown at higher magnification. Original magnifications: ×5 (**A**, **B**, **top**); ×40 (**A**, **B**, **bottom**).

phorylation. As described for rTg4510, the first disease associated epitope detected in rTg3696AB was CP-13 (pSer^{202}), which labeled copious numbers of neurons throughout the hippocampus and cortex. At this early stage of pathology in rTg4510, CP-13-positive labeling is closely mirrored by conformational-dependent antibody MC-1. However, at 4 months of age MC-1-positive neurons were only observed in the CA1 subdivision of the hippocampus, suggesting that the conformational change occurs after phosphorylation at Ser^{202}.

Equally, the age at which pretangle-specific tau epitopes could be detected lagged behind that previously observed in rTg4510. AT-8 (pSer^{202} and pThr^{205}) and PG-5 (pSer^{409}) positive neurons were detected throughout the forebrain at 11 months of age. In parallel to Aβ plaque observations, this seemed to be an important time point because the number of AT-8 and PG-5 positive neurons increased substantially between 11 and 13 months of age. That the cortical tauopathy precedes that in the hippocampus reveals that tau pathology in rTg3696AB more closely reflects that observed in frontotemporal dementia than AD. This is most likely dependent on the frontotemporal dementia-linked mutation in tau and supports previous observations in rTg4510, in the absence of plaque pathology.[26]

That these pathological biochemical changes inevitably lead to the formation of mature argyrophilic NFTs was confirmed using Bielschowsky silver stain. At 13 months of age histological processing revealed abundant NFTs and senile plaques throughout the forebrain. It was also apparent, at this age, that these AD-related pathologies were associated with tissue atrophy and neuronal loss. Consistent with the forebrain-specific CaMKII promoter system, neurodegeneration was most evident in the hippocampus and cortex. Most striking neuronal loss occurred in the CA1, the hippocampal subdivision that was most vulnerable to the formation of NFTs. A decrease in neuronal density was clearly observed in mice aged older than 11 months, however it is likely that loss of neurons commenced in younger animals. Neuronal loss was also obvious in the molecular layer of the dentate gyrus, a cell layer in which NFTs were rarely observed, suggesting multiple mechanisms of neuronal death.[40] Increased vulnerability of the dentate gyrus may be associated with loss of input from the entorhinal cortex, a brain region that experiences severe degeneration. Neuronal loss observations were supported when tissue was processed with hematoxylin. These images revealed specific localized areas of neurodegeneration associated with the formation of senile plaques.[2]

Previous groups have created nonregulatable transgenic models expressing both APP and tau that develop Aβ plaque and NFT lesions. These mice have yielded interesting findings with regard to the influence one pathology exerts on the other. In 2001, Lewis and colleagues[21] crossed Tg2576 with JNPL3 mice (tau$_{P301L}$). In this study, the authors reported an increase in NFT pathology that was not associated with a change in Aβ plaque deposition.[21] This finding was supported by a recent report in APP23 × B6/P301 mice specifically citing increased tau pathology in close proximity to plaques.[41] Other groups observed an increase in both Aβ deposition and NFT pathology in Tg2576 crossed with mice harboring three mutations in tau (VLW; G272V, P301L and R406W).[37] In this model, an increase in tau phosphorylation was hypothesized to reciprocate a link between the two pathological cascades.[42] Unfortunately, a clear demonstration of the molecular connection between Aβ plaques and NFTs remains enigmatic. However, findings in the 3xTg-AD model (APP $_{SWE}$, PS1$_{M146V}$ and tau$_{P301L}$) support the long held hypothesis that Aβ deposition precedes NFT formation because tangle pathology is delayed in 2xTg-AD mice (PS1$_{M146V}$ and tau$_{P301L}$).[43] Although these models are useful tools in elucidating the underlying pathological mechanisms one must not forget the limitation of transgenic studies because findings are strongly influenced by the specific conditions used (ie, mutation, promoter, expression levels. and mouse genetic background).

The ultimate goal of this study was to create a mouse model of the two cardinal AD features, plaques and tangles, in which transgene expression was regulatable. To achieve this, we generated mice with co-integrated TRE-APP$_{NLI}$ and TRE-tau$_{P301L}$ transgene arrays. Thus, all mice harboring both the responder and activator transgene express both transgenic human APP and tau. The

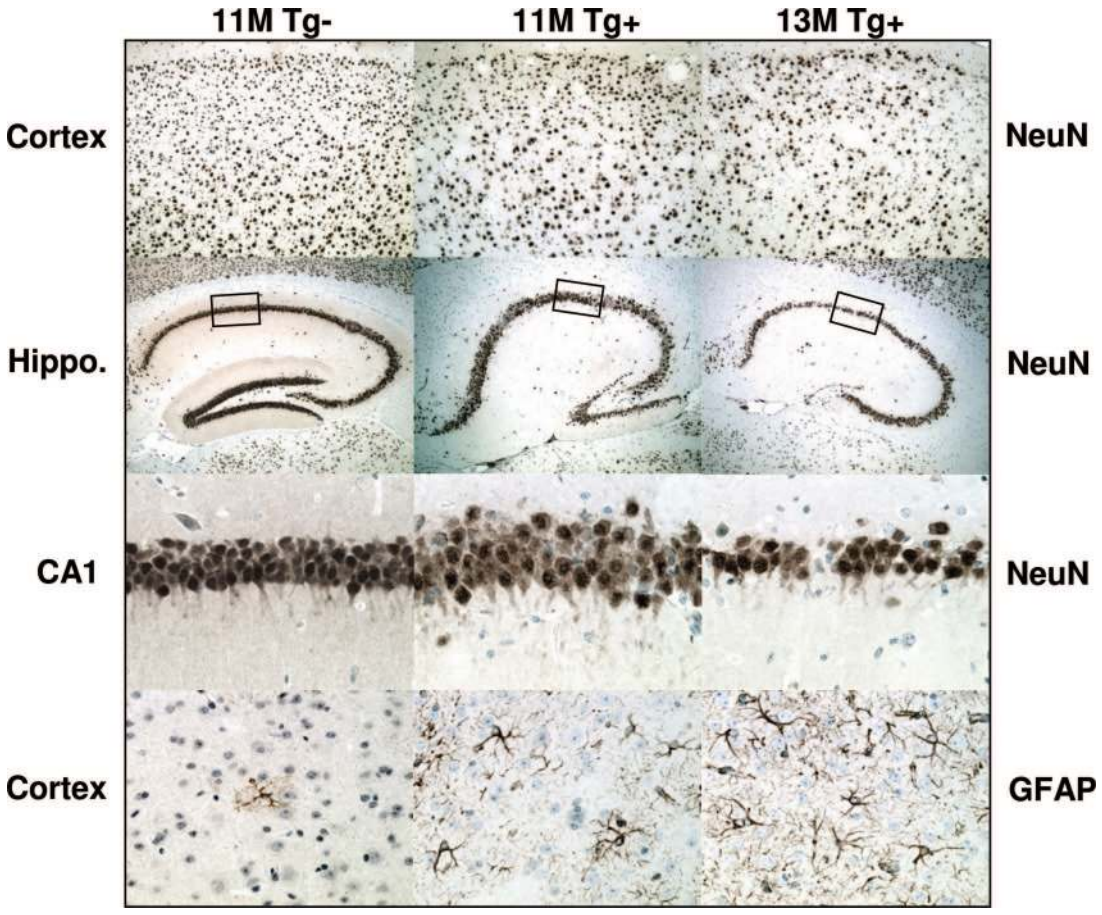

Figure 9. Neuronal loss and astrogliosis in aged rTg3696AB mice. Tissue was processed with neuron-specific antibody NeuN. Images indicate substantial loss of neurons in rTg3696AB mice between 11 and 13 months. Representative photomicrographs depict cortex (**top**), hippocampus, and CA1 hippocampal subdivision (**middle**) after processing with NeuN. In parallel, GFAP was used to detect glia cells (**bottom**). Original magnifications: ×10 (**top**); ×5 (**top middle**); ×40 (**bottom middle** and **bottom**).

resulting model closely mimics the human disease of interest because the mice develop plaque and tangle pathologies that are associated with neurodegeneration. Although we have not yet behaviorally characterized this novel transgenic line, one would confidently predict that pathology will be accompanied with impairments in memory function. However, we must acknowledge the limitation that one can achieve pathology only by expressing three transgene arrays simultaneously, ie, i) CK-tTA transgene; ii) the A responder line harboring a TRE-APP_{NLI} and TRE-tau_{P301L} transgene array; and iii) the B responder line harboring a different TRE-APP_{NLI} and TRE-tau_{P301L} transgene array. Compared to rTg3696AB, rTg3696A mice express approximately half the levels of APP_{NLI} and TRE-tau_{P301L} (~1.5 units). This observation suggests a nonlinear threshold of transgenic APP/tau burden that the brain is able to manage, as the rTg3696A line showed no pathology when examined up to 24 months of age.

The regulatable nature of transgene expression in rTg3696AB facilitates studies designed to test experimental hypotheses using transgene suppression. Future experiments using rTg3696AB will use transgene suppression to mimic therapeutic strategies that target plaques and tangles. The effect of transgene suppression of the progression of pathology with regard to memory function will be most interesting. Recent studies in rTg4510 showed that NFT pathology continued after substantial transgene suppression.[27] Furthermore, NFT pathology progressed concurrently with a significant improvement in retention of spatial reference memory. These surprising data suggested that NFTs were not primarily responsible for cognitive impairment in rTg4510 and may in fact represent an attempted neuroprotective sequestration of tau. Whether a similar recovery is possible in the presence of Aβ plaque deposits is unknown. Moreover, it was previously shown in a regulatable $APP_{SWE/IND}$ model, that plaques are extremely stable structures that remained in the brain during a 6-month period of almost complete transgene suppression.[36] However, the effects of transgene suppression on Aβ plaque deposition and memory retention remain to be determined.

Acknowledgments

We thank L. Kotilinek, L. Kemper, M. Schmidt, and J. Starks for technical expertise; P. Sharpe for secretarial assistance; Dr. P. Davies for the generous gift of antibodies; and Dr. E. Kandel for the generous donation of activator mice.

References

1. Selkoe DJ: Cell biology of protein misfolding: the examples of Alzheimer's and Parkinson's diseases. Nat Cell Biol 2004, 6:1054–1061
2. Knowles RB, Wyart C, Buldyrev SV, Cruz L, Urbanc B, Hasselmo ME, Stanley HE, Hyman BT: Plaque-induced neurite abnormalities: implications for disruption of neural networks in Alzheimer's disease. Proc Natl Acad Sci USA 1999, 96:5274–5279
3. Urbanc B, Cruz L, Le R, Sanders J, Ashe KH, Duff K, Stanley HE, Irizarry MC, Hyman BT: Neurotoxic effects of thioflavin S-positive amyloid deposits in transgenic mice and Alzheimer's disease. Proc Natl Acad Sci USA 2002, 99:13990–13995
4. D'Amore JD, Kajdasz ST, McLellan ME, Bacskai BJ, Stern EA, Hyman BT: In vivo multiphoton imaging of a transgenic mouse model of Alzheimer disease reveals marked thioflavine-S-associated alterations in neurite trajectories. J Neuropathol Exp Neurol 2003, 62:137–145
5. Lombardo JA, Stern EA, McLellan ME, Kajdasz ST, Hickey GA, Bacskai BJ, Hyman BT: Amyloid-beta antibody treatment leads to rapid normalization of plaque-induced neuritic alterations. J Neurosci 2003, 23:10879–10883
6. Brendza RP, Bacskai BJ, Cirrito JR, Simmons KA, Skoch JM, Klunk WE, Mathis CA, Bales KR, Paul SM, Hyman BT, Holtzman DM: Anti-Abeta antibody treatment promotes the rapid recovery of amyloid-associated neuritic dystrophy in PDAPP transgenic mice. J Clin Invest 2005, 115:428–433
7. Spires TL, Meyer-Luehmann M, Stern EA, McLean PJ, Skoch J, Nguyen PT, Bacskai BJ, Hyman BT: Dendritic spine abnormalities in amyloid precursor protein transgenic mice demonstrated by gene transfer and intravital multiphoton microscopy. J Neurosci 2005, 25:7278–7287
8. Meyer-Luehmann M, Spires-Jones TL, Prada C, Garcia-Alloza M, de Calignon A, Rozkalne A, Koenigsknecht-Talboo J, Holtzman DM, Bacskai BJ, Hyman BT: Rapid appearance and local toxicity of amyloid-beta plaques in a mouse model of Alzheimer's disease. Nature 2008, 451:720–724
9. Stern EA, Bacskai BJ, Hickey GA, Attenello FJ, Lombardo JA, Hyman BT: Cortical synaptic integration in vivo is disrupted by amyloid-beta plaques. J Neurosci 2004, 24:4535–4540
10. Roher AE, Chaney MO, Kuo YM, Webster SD, Stine WB, Haverkamp LJ, Woods AS, Cotter RJ, Tuohy JM, Krafft GA, Bonnell BS, Emmerling MR: Morphology and toxicity of Abeta-(1-42) dimer derived from neuritic and vascular amyloid deposits of Alzheimer's disease. J Biol Chem 1996, 271:20631–20635
11. Lambert MP, Barlow AK, Chromy BA, Edwards C, Freed R, Liosatos M, Morgan TE, Rozovsky I, Trommer B, Viola KL, Wals P, Zhang C, Finch CE, Krafft GA, Klein WL: Diffusible, nonfibrillar ligands derived from Abeta1-42 are potent central nervous system neurotoxins. Proc Natl Acad Sci USA 1998, 95:6448–6453
12. Hartley DM, Walsh DM, Ye CP, Diehl T, Vasquez S, Vassilev PM, Teplow DB, Selkoe DJ: Protofibrillar intermediates of amyloid beta-protein induce acute electrophysiological changes and progressive neurotoxicity in cortical neurons. J Neurosci 1999, 19:8876–8884
13. Bitan G, Lomakin A, Teplow DB: Amyloid beta-protein oligomerization: prenucleation interactions revealed by photo-induced cross-linking of unmodified proteins. J Biol Chem 2001, 276:35176–35184
14. Lashuel HA, Hartley D, Petre BM, Walz T, Lansbury PT Jr: Neurodegenerative disease: amyloid pores from pathogenic mutations. Nature 2002, 418:291
15. Hoshi M, Sato M, Matsumoto S, Noguchi A, Yasutake K, Yoshida N, Sato K: Spherical aggregates of beta-amyloid (amylospheroid) show high neurotoxicity and activate tau protein kinase I/glycogen synthase kinase-3beta. Proc Natl Acad Sci USA 2003, 100:6370–6375
16. Barghorn S, Nimmrich V, Striebinger A, Krantz C, Keller P, Janson B, Bahr M, Schmidt M, Bitner RS, Harlan J, Barlow E, Ebert U, Hillen H: Globular amyloid beta-peptide oligomer—a homogenous and stable neuropathological protein in Alzheimer's disease. J Neurochem 2005, 95:834–847
17. Lesné S, Koh MT, Kotilinek L, Kayed R, Glabe CG, Yang A, Gallagher M, Ashe KH: A specific amyloid-beta protein assembly in the brain impairs memory. Nature 2006, 440:352–357
18. Walsh DM, Klyubin I, Fadeeva JV, Cullen WK, Anwyl R, Wolfe MS, Rowan MJ, Selkoe DJ: Naturally secreted oligomers of amyloid beta protein potently inhibit hippocampal long-term potentiation in vivo. Nature 2002, 416:535–539
19. Cheng IH, Scearce-Levie K, Legleiter J, Palop JJ, Gerstein H, Bien-Ly N, Puolivali J, Lesne S, Ashe KH, Muchowski PJ, Mucke L: Accelerating amyloid-beta fibrillization reduces oligomer levels and functional deficits in Alzheimer disease mouse models. J Biol Chem 2007, 282:23818–23828
20. Ishihara T, Hong M, Zhang B, Nakagawa Y, Lee MK, Trojanowski JQ, Lee VM: Age-dependent emergence and progression of a tauopathy in transgenic mice overexpressing the shortest human tau isoform. Neuron 1999, 24:751–762
21. Lewis J, Dickson DW, Lin WL, Chisholm L, Corral A, Jones G, Yen SH, Sahara N, Skipper L, Yager D, Eckman C, Hardy J, Hutton M, McGowan E: Enhanced neurofibrillary degeneration in transgenic mice expressing mutant tau and APP. Science 2001, 293:1487–1491
22. Lim F, Hernandez F, Lucas JJ, Gomez-Ramos P, Moran MA, Avila J: FTDP-17 mutations in tau transgenic mice provoke lysosomal abnormalities and Tau filaments in forebrain. Mol Cell Neurosci 2001, 18:702–714
23. Andorfer C, Kress Y, Espinoza M, de Silva R, Tucker KL, Barde YA, Duff K, Davies P: Hyperphosphorylation and aggregation of tau in mice expressing normal human tau isoforms. J Neurochem 2003, 86:582–590
24. Terwel D, Lasrado R, Snauwaert J, Vandeweert E, Van Haesendonck C, Borghgraef P, Van Leuven F: Changed conformation of mutant Tau-P301L underlies the moribund tauopathy, absent in progressive, nonlethal axonopathy of Tau-4R/2N transgenic mice. J Biol Chem 2005, 280:3963–3973
25. Mocanu MM, Nissen A, Eckermann K, Khlistunova I, Biernat J, Drexler D, Petrova O, Schonig K, Bujard H, Mandelkow E, Zhou L, Rune G, Mandelkow EM: The potential for beta-structure in the repeat domain of tau protein determines aggregation, synaptic decay, neuronal loss, and coassembly with endogenous Tau in inducible mouse models of tauopathy. J Neurosci 2008, 28:737–748
26. Ramsden M, Kotilinek L, Forster C, Paulson J, McGowan E, SantaCruz K, Guimaraes A, Yue M, Lewis J, Carlson G, Hutton M, Ashe KH: Age-dependent neurofibrillary tangle formation, neuron loss, and memory impairment in a mouse model of human tauopathy (P301L). J Neurosci 2005, 25:10637–10647
27. SantaCruz K, Lewis J, Spires T, Paulson J, Kotilinek L, Ingelsson M, Guimaraes A, DeTure M, Ramsden M, McGowan E, Forster C, Yue M, Orne J, Janus C, Mariash A, Kuskowski M, Hyman B, Hutton M, Ashe KH: Tau suppression in a neurodegenerative mouse model improves memory function. Science 2005, 309:476–481
28. Mayford M, Bach ME, Huang YY, Wang L, Hawkins RD, Kandel ER: Control of memory formation through regulated expression of a CaMKII transgene. Science 1996, 274:1678–1683
29. Borchelt DR, Davis J, Fischer M, Lee MK, Slunt HH, Ratovitsky T, Regard J, Copeland NG, Jenkins NA, Sisodia SS, Price DL: A vector for expressing foreign genes in the brains and hearts of transgenic mice. Genet Anal 1996, 13:159–163
30. Hsiao K, Chapman P, Nilsen S, Eckman C, Harigaya Y, Younkin S, Yang F, Cole G: Correlative memory deficits. Abeta elevation, and amyloid plaques in transgenic mice. Science 1996, 274:99–102
31. Mullan M, Houlden H, Windelspecht M, Fidani L, Lombardi C, Diaz P, Rossor M, Crook R, Hardy J, Duff K, Mullan M, Houlden H, Windelspecht M, Fidani L, Lombardi C, Diaz P, Rossor M, Crook R, Hardy J, Duff K, Crawford F: A locus for familial early-onset Alzheimer's disease on the long arm of chromosome 14, proximal to the alpha 1-antichymotrypsin gene. Nat Genet 1992, 2:340–342
32. Goate A, Chartier-Harlin MC, Mullan M, Brown J, Crawford F, Fidani L, Giuffra L, Haynes A, Irving N, James L, Goate A, Chartier-Harlin M-C, Mullan M, Brown J, Crawford F, Fidani L, Giuffra L, Haynes A, Irving N, James L, Mant R, Newton P, Rooke K, Roques P, Talbot C, Pericak-Vance M, Roses A, Williamson R, Rossor M, Owen M, Hardy J: Segregation of a missense mutation in the amyloid precursor protein gene with familial Alzheimer's disease. Nature 1991, 349:704–706
33. Gossen M, Bujard H: Tight control of gene expression in mammalian cells by tetracycline-responsive promoters. Proc Natl Acad Sci USA 1992, 89:5547–5551
34. Borchelt DR, Ratovitski T, van Lare J, Lee MK, Gonzales V, Jenkins NA, Copeland NG, Price DL, Sisodia SS: Accelerated amyloid deposition in the brains of transgenic mice coexpressing mutant

presenilin 1 and amyloid precursor proteins. Neuron 1997, 19:939–945
35. Kawarabayashi T, Younkin LH, Saido TC, Shoji M, Ashe KH, Younkin SG: Age-dependent changes in brain, CSF, and plasma amyloid (beta) protein in the Tg2576 transgenic mouse model of Alzheimer's disease. J Neurosci 2001, 21:372–381
36. Jankowsky JL, Slunt HH, Gonzales V, Savonenko AV, Wen JC, Jenkins NA, Copeland NG, Younkin LH, Lester HA, Younkin SG, Borchelt DR: Persistent amyloidosis following suppression of Abeta production in a transgenic model of Alzheimer disease. PLoS Med 2005, 2:1318–1333
37. Ribé EM, Perez M, Puig B, Gich I, Lim F, Cuadrado M, Sesma T, Catena S, Sanchez B, Nieto M, Gomez-Ramos P, Moran MA, Cabodevilla F, Samaranch L, Ortiz L, Perez A, Ferrer I, Avila J, Gomez-Isla T: Accelerated amyloid deposition, neurofibrillary degeneration and neuronal loss in double mutant APP/tau transgenic mice. Neurobiol Dis 2005, 20:814–822
38. Hutton M, Lendon CL, Rizzu P, Baker M, Froelich S, Houlden H, Pickering-Brown S, Chakraverty S, Isaacs A, Grover A, Hackett J, Adamson J, Lincoln S, Dickson D, Davies P, Petersen RC, Stevens M, de Graaff E, Wauters E, van Baren J, Hillebrand M, Joosse M, Kwon JM, Nowotny P, Che LK, Norton J, Morris JC, Reed LA, Trojanowski J, Basun H, Lannfelt L, Neystat M, Fahn S, Dark F, Tannenberg T, Dodd PR, Hayward N, Kwok JB, Schofield PR, Andreadis A, Snowden J, Craufurd D, Neary D, Owen F, Oostra BA, Hardy J, Goate A, van Swieten J, Mann D, Lynch T, Heutink P: Association of missense and 5′-splice-site mutations in tau with the inherited dementia FTDP-17. Nature 1998, 393:702–705
39. Götz J, Chen F, van Dorpe J, Nitsch RM: Formation of neurofibrillary tangles in P301l tau transgenic mice induced by Abeta 42 fibrils. Science 2001, 293:1491–1495
40. Spires TL, Orne JD, SantaCruz K, Pitstick R, Carlson GA, Ashe KH, Hyman BT: Region-specific dissociation of neuronal loss and neurofibrillary pathology in a mouse model of tauopathy. Am J Pathol 2006, 168:1598–1607
41. Bolmont T, Clavaguera F, Meyer-Luehmann M, Herzig MC, Radde R, Staufenbiel M, Lewis J, Hutton M, Tolnay M, Jucker M: Induction of tau pathology by intracerebral infusion of amyloid-beta-containing brain extract and by amyloid-beta deposition in APP x Tau transgenic mice. Am J Pathol 2007, 171:2012–2020
42. Pérez M, Ribe E, Rubio A, Lim F, Moran MA, Ramos PG, Ferrer I, Isla MT, Avila J: Characterization of a double (amyloid precursor protein-tau) transgenic: tau phosphorylation and aggregation. Neuroscience 2005, 130:339–347
43. Oddo S, Caccamo A, Shepherd JD, Murphy MP, Golde TE, Kayed R, Metherate R, Mattson MP, Akbari Y, LaFerla FM: Triple-transgenic model of Alzheimer's disease with plaques and tangles: intracellular Abeta and synaptic dysfunction. Neuron 2003, 39:409–421